# A Human-like Walking Gait Simulator for Pedestrian Dead Reckoning Navigation

Mahdi Abid, Valérie Renaudin, Thomas Robert, Yannick Aoustin, Eric Le-Carpentier

# A Human-like Walking Gait Simulator for Pedestrian Dead Reckoning Navigation

Mahdi Abid[1,3], Valerie Renaudin[1], Thomas Robert[2,3], Yannick Aoustin[4], Eric Le-Carpentier[4]
[1]IFSTTAR, GEOLOC Laboratory, Route de Bouaye CS4, 44344 Bouguenais, France
[2]Univ. Lyon, Université Claude Bernard Lyon 1, France
[3]IFSTTAR, LBMC UMR_T9406, 69622 Lyon, France
[4]LS2N, UMR 6004, École Centrale de Nantes, Université de Nantes, France
E-mails: {valerie.renaudin, thomas.robert}@ifsttar.fr, Yannick.Aoustin@univ-nantes.fr, eric.le-carpentier@ec-nantes.fr

***Abstract*—Pedestrian dead reckoning (PDR) is one of the most employed strategies to process inertial signals collected with a handheld device for autonomous indoor positioning. This strategy is based on step length models that usually combine step characteristics with some physiological parameters. These models are calibrated with experimental data for each user. However, many physiological conditions are affecting the walking gait even for steady walking. Therefore, frequent calibration is needed to cope with walking pattern variations. Moreover, PDR models are not adapted to high walking velocities and to the specific walking patterns of some populations like elderly people and pathological cases. In light of these limitations, the modeling of human walking, which considers the induced arm swinging behavior, is needed for improving self-contained inertial indoor navigation. In this paper, a human-like walking model is developed in order to represent and study the correlations between the hand acceleration and gait characteristics. Experimental data were collected from motion capture experiments on one healthy subject in order to validate the model. Results show that the model fitted to the test subject reproduces the walking features found in experiments, as well as the same tendencies in function of the walking velocity.**

## I. Introduction

Nowadays, more wearable devices are introduced for observing and supporting personal mobility in order to ensure accurate indoor localization and displacement features extraction. The study of users mobility is mainly performed using GNSS (Global Navigation Satellites Systems) data whose results are often biased in indoor spaces since radio signals are weakened by infrastructures and dynamic obstacles [1]. This results in loss of information on human movement and consequently in a less accurate positioning solution, or even solution loss.

An alternative solution consists in using signals collected with inertial sensors [2] since these data are available regardless of local infrastructures. This approach led to improvement in assisting personal mobility. Pedestrian Dead Reckoning (PDR) is one of the most used strategies based on signals collected with handheld devices. This process combines estimated distance and direction to determine a displacement relative to a known starting position. Nevertheless, the complex nature of hand motions performed by handheld devices users during their displacement makes the estimation of walking directions and distances more complex. Contrary to sensors attached to foot or waist, walking pattern is not directly sensed when using handheld devices. Parametric models have been used to address this issue. They estimate step length by combining step characteristics (step frequency) and physiological parameters (user's height) [3], [4], [5].

Most of the current step length models show some limits. They are only adapted to the common human gait (small variation of step length and frequency through different users). The step length estimation is less accurate when it comes to more varied or particular walking gaits [5] (e.g. pathological cases). Moreover, they assume the periodicity of gait pattern regardless of some conditions like fatigue and the weight of a carried mass [6]. Tiny deviation in each step results in high cumulative error in the final positioning result. Consequently, frequent calibrations based on large-scale empirical data are needed to tune existing step length models. For more positioning accuracy, we present a numerical tool aiming at simulating human walking gait, taking into account the arm swing that is correlated with leg motion [7]. This model is capable of generating all sorts of gaits, because the result depends on many parameters such as walking velocity and the physical properties of the user. This simulation based approach enables to find out the objective correlations between step characteristics (speed, step characteristics, etc.) and acceleration data without the need for multiple experiments that are costly to carry out and do not cover the variety of human gait patterns. In this paper, this model is fitted to one test subject and evaluated with motion capture data using chosen salient variables. Preliminary results show that the model reproduces the same features of human walking found in experiments, as well as the same tendencies of acceleration data in terms of gait velocity.

The paper is organized as follows. Section II introduces the dedicated human-like gait motion generator. Section III details the experimental evaluation procedure of the proposed gait model. Evaluation results are discussed in Section IV. Finally, Section V concludes this paper.

## II. Presentation of human gait model

### A. Proposed 3D biped model

A previous study showed that modeling in 3D is needed to better simulate human walking [8]. For instance, the pelvis

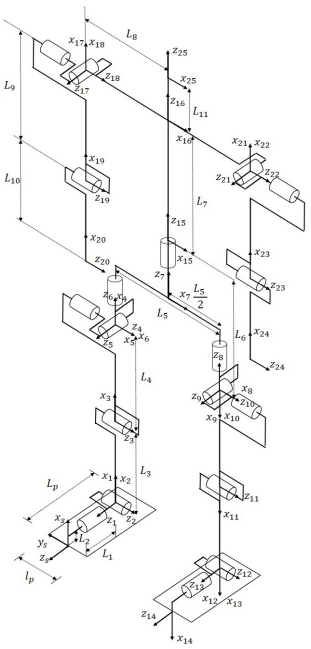

FIG. 1 – *The local frames of the 3D biped according to Denavit-Hartenberg convention.*

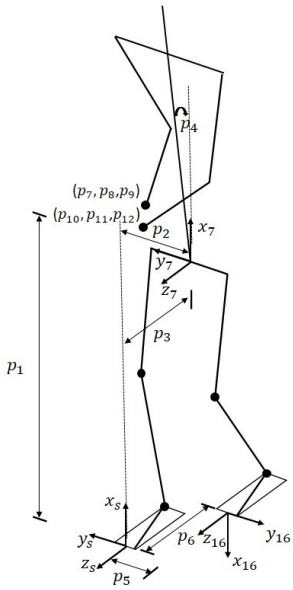

FIG. 2 – *The 12 geometric parameters determining the initial biped's configuration at DS: Six parameters for arms configuration, four parameters for pelvis position and orientation, and two parameters for step characteristics.*

rotation in the transverse plane should be modeled as it contributes to the step length [9], [10].

The proposed anthropomorphic model is illustrated in Fig. 1. All links are considered as rigid and connected by frictionless joints. All articulations are revolute. The degrees of freedom (DOFs) of joints are chosen based on human walking analysis found in [11], [12]. The 19-DOF biped is composed of a head-neck, torso, pelvis, two identical two-link arms with three DOFs, and two identical three-link legs with three DOF spherical hips ended with feet bodies. Each knee and elbow contains a one DOF revolute joint. The trunk and pelvis are connected by a revolute joint with one DOF.

To adjust this biped to a test subject, body segment inertial parameters must be estimated. For each link, they consist in its mass, its inertias and its COM position in the body referential. The regressions of Dumas [13], based on the extensive data of McConville [14] and de Young [15] (Mass distribution and anthropometric characteristics of adult men and women) are used. In addition, segments lengths are estimated according to the anatomical definition reported by [13].

### *B. Definition of gait cycle*

The biped steady state gait is a periodical phenomenon whose unitary element is a gait cycle (GC also named a stride). It is defined between by two consecutive step events of the same foot (in this study we consider the mid-flat foot). It consists of the succession of two consecutive steps. It starts with an event relative to one foot (the end of the flat foot phase). A gait cycle thus includes two double support (DS) phases and two single support (SS) phases. In this study, the DS phases are supposed to be instantaneous. Moreover, we assumed that steps are symmetrical. The optimization problem was solved for a single step. The other step is generated using inversion matrix describing the exchange of role of legs and arms.

The gait motion over a step in a time interval [0, $T$], is defined by the following set of parameters:

- The intermediate configurations in SS: (n-2)×19 parameters, where n is the number of uniformly spaced time knots, n=4 in this study;
- The final joint velocity of the biped just before the impact: 19 parameters;
- The parameters of DS configuration (see Fig. 2): 12 parameters.

The above-mentioned parameters are the subjects of a cost functional minimization in order to extract a unique solution. The optimal values of these parameters are obtained using the following optimization process.

### *C. Optimization process*

The nonlinear constrained problem is solved with a parametric optimization algorithm using *SQP* method (Sequential Quadratic Programming) [16].

*1) Joint Trajectory Interpolation:* Spline functions are used in order to interpolate joint motion histories profile from the control points that are optimized during the optimization process.

*2) Cost function:* In our modeling problem, we aim at minimizing the joint actuators energy dissipated over a step of duration $T$ to travel the distance $d$. We consider a cost functional $C_\Gamma$ that is the integral of the norm of joint torques, approximated by a finite sum of torques function values at the chosen time samples [17]:

$$C_\Gamma = \frac{1}{d}\int_0^T \mathbf{\Gamma}(t)^\top \mathbf{\Gamma}(t)\ \mathrm{d}t \tag{1}$$

where $\mathbf{\Gamma}$ is the vector of joint torques.
Additionally, a potential cost functional involves the deviation of the trunk segment from upright position [18] which is amounted to the following function:

$$C_{upright} = \int_0^T (\boldsymbol{p}_7(t) - \boldsymbol{p}_h(t)) \cdot \boldsymbol{g}\ \mathrm{d}t \tag{2}$$

where $\boldsymbol{p}_h$ is the cartesian coordinates of the hips middle point, $\boldsymbol{p}_7$ is the cartesian coordinates of the $7^{\text{th}}$ Cervicale corresponding in our biped model to the origin $O_{16}$, $\boldsymbol{g}$ is the gravity vector and the operator $\cdot$ denotes the scalar product.

*3) Constraints:* Several constraints are imposed to have a human-like GC:

- Joint torques, rates and positions must not exceed their limits;
- In DS, a constraint keeps the landing foot from occupying simultaneously the same ground area with the stance foot;
- During swing, additional constraints on the position of the four corners of the swing foot are imposed in order to avoid collision between the swing leg and the stance leg or the ground;
- Ground reaction for SS and the impact forces in DS must be inside a friction cone of a coefficient $\mu$ to ensure stability, and must be directed upward to avoid stance foot's take-off;
- Zero Moment Point (ZMP) needs to be constrained inside the base of support (BoS) defined by the four corners of the support foot to maintain balance in dynamic walking;
- Zero Yawing Moment (ZYM) constraint [18] is added in order to generate contralateral swing of the arms. It consists in constraining the normal component of moment due to the inertial and gravity force about the ZMP under a small upper bound of magnitude (= 0.1 N.m in this study). Consequently, the yawing moment induced by leg motion is cancelled out by that of ipsilateral arm motion leading to self-equilibration of this moment component.

## III. Experimental evaluation procedure

Experimental data were collected in order to check the validity of the suggested human gait simulator. These data were compared to simulation outputs based on chosen salient variables.

### A. Data collection

A 25-year-old healthy subject, 1.84 m tall and weighing 85 kg, participated in motion capture experiments after providing a written informed consent. 17 reflective markers were placed on his feet, legs, pelvis, trunk, head, arms, forearms and hands. While the subject walked on a treadmill, an 8-camera ART IR tracking system recorded the displacement of the markers in three-dimensional space at 60 Hz (cf. Fig. 3). Inertial data were also collected using an ULISS (Ubiquitous Localization Unit with Inertial Sensors and Satellites) device [19] held by the right hand of the subject. It comprises 9 degrees of freedom inertial mobile unit, a high sensitivity GNSS (HSGNSS) receiver and antenna, a memory card, and a battery. Inertial sensors and magnetometers provide measurements at a 200 Hz frequency. Optical markers' assembly was tapped to this device (cf. Fig. 4) in order to project sensor's data in motion lab frame.

The subject completed three trials. For each trial, he was asked to walk on the treadmill for 100 continuous strides with the IMU unit in the right hand. Three different treadmill's belt speeds were used (one per trial), corresponding to a slow ($V_1$, 1 m/s), comfortable ($V_2$, 1.39 m/s) and high ($V_3$, 1.61 m/s) walking speed. For each trial, data record started only after the participant had reached a steady state at the corresponding walking speed.

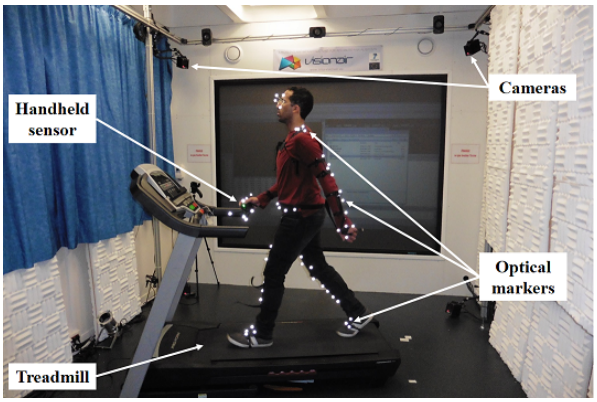


FIG. 3 – *Experimental setup*

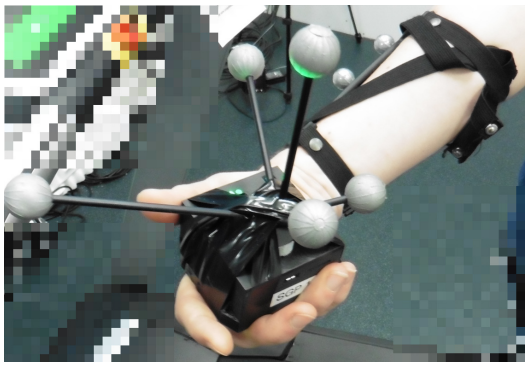

FIG. 4 – *ULISS device with an optical markers' assembly*

Walking on a treadmill results in a more consistent and symmetric gait pattern with respect to overground walking [20]. Yet, the use of a treadmill was preferred to test straight walking for several steady walking speeds. Moreover, this alternative allows accurate measurements of the markers' positions in order to derive gait features.

### B. Salient variables

For experimental validation of our gait model, we choose determinant variables of human walking as well as some acceleration data related items that are usually utilized in current step length estimation models:

- Kinematics of the arm: Arcs of shoulder and elbow motion in the sagittal plane estimated from the positions of the markers linked to the right hand, arm, forearm and trunk.
- COM mediolateral and vertical displacements: These data were estimated from the pelvis markers displacement, since we assume that the pelvis reproduce the same motion as the whole body COM.
- Step characteristics: step length, width and cadence were calculated. Given the walking velocity, step length was calculated from duration between two consecutive step events from foot contact to contralateral foot contact. Stride width was the linear distance between feet markers position from foot contact to contralateral foot contact along the lateral direction. Cadence was calculated as steps per minute. Mean values across 50 steps were considered for these variables.
- Some items of acceleration data in vertical direction:
  - The magnitude $M_a$, as involved in Kim model [21], which is defined by:

$$M_a = \frac{\sum_{i=1}^{N} |a_i|}{N} \tag{3}$$

    where $N$ is the number of sampling points in the stride, and $a_i$ stands for the vertical acceleration of the $i^{\text{th}}$ point.
  - The difference between peak and trough values used in Weinberg Model [22].
  - The variance defined as the average of the squared differences from the mean, used in [4].

  Acceleration data were calculated after compensating the gravity acceleration from raw data. Acceleration data were projected in the motion lab reference frame knowing the fixed rotation matrix between IMU frame and the frame of the cluster tapped to it.

### C. Data processing

*1) Synchronization with simulation data:* In order to compare salient variables profiles from both simulation and experimental data, we resampled stride time profiles over 100 points from 1 to 100, where 1 denotes the beginning of the GC while 100 marks its end (see Fig. 5). Note that while DS phases last nearly 20% of the GC [11], they were considered as instantaneous in the simulation.

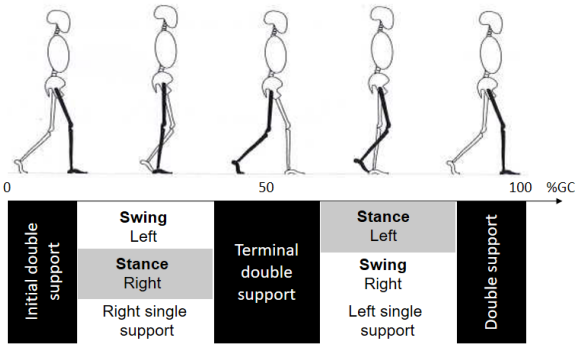


FIG. 5 – *The subdivisions of GC [11].*

*2) Strides detection:* The Zero Velocity Detection (ZVD) method was used to detect step events of both feet. It is based on an acceleration moving variance detector and it searches for the periods when the foot-mounted cluster of markers is stationary [23]. Step events detected with this method thus corresponded to the end of the flat ipsilateral foot phase. In our study, it is applied to acceleration data obtained by double differentiating the feet markers' positions. In order to remove the noise induced by the derivation, the data are low-pass filtered with a zero-phase forward and reverse second order Butterworth filter with a cut-off frequency of 10 Hz.

The variance of the norm of the acceleration vector is calculated over a sliding window and compared to a threshold. The sliding window is less wide for higher gait speeds since stationary phase gets shorter. The variance threshold was adjusted so that stationary phases for each GC are detected.

*3) Averaged pattern over a stride:* After corresponding data for each stride, stride-specific patterns need to be synchronized in time. First, data were interpolated using splines and then we used Dynamic Time Warping (DTW) [24] to align different signals in time. This transformation allows to estimate the average GC profile for each variable. The average value of a variable A is given by:

$$A_i = \frac{1}{N_s} \sum_{k=1}^{N_s} A_{ik} \tag{4}$$

where $i$ denotes an index within the stride cycle, $k$ is the stride index, and $N_s$ is the total number of consecutive stride profiles.

## IV. RESULTS

### A. Natural aspects of walking

In this section, GC profiles of salient variables related to natural aspects of walking are illustrated for both experimental and simulation cases, by solid and dashed curves respectively.

*1) Arm motion:* Fig. 6 and Fig. 7 provide right shoulder and elbow motion in the sagittal plane during GC. The same patterns of arcs of motion are obtained for both simulation and experimental approaches. The shoulder reaches his maximum extension (20°) during initial DS phase and then flexes to a peak position in terminal DS. After holding this position, the shoulder extends through the next SS phase. In simulation,

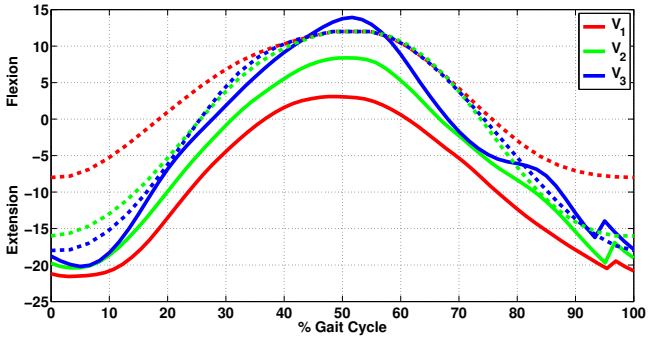


FIG. 6 – *Arcs of shoulder motion profile during arm swing for a GC. Solid line for experimental data, dashed line for simulation data.*

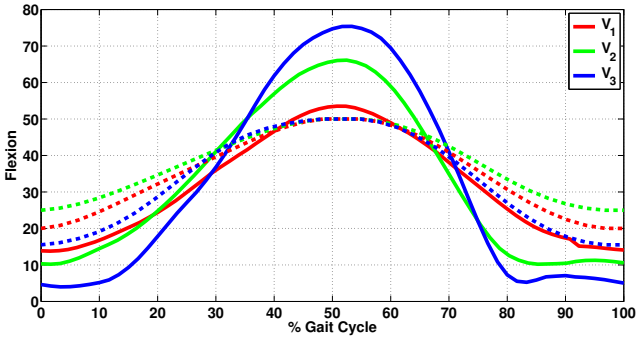


FIG. 7 – *Arcs of elbow motion profile during arm swing for a GC. Solid line for experimental data, dashed line for simulation data.*

although the peak flexion remains the same, the total arc of motion increases with faster gait velocities with values close to experimental ones. A similar pattern is obtained for the elbow. Flexion arc occurs in ipsilateral foot stance phase and extension arc is performed during ipsilateral foot swing.

*2) COM displacement:* The gait model reproduced the same displacement patterns in both lateral and vertical directions (Fig. 8 and Fig. 9). The COM is displaced following a double sinusoidal path in vertical direction and single sinusoidal path in lateral direction. The lateral displacement is increased for low speeds while vertical displacement is greater for faster velocities. In DS phases, neutral position in lateral direction and minimum vertical position of the COM are reached. Difference in lateral displacement magnitudes between both approaches are due to the difference between step width values since lateral displacement depends on walking base [9].

### B. Step characteristics

Table I provides step characteristics values over the three walking velocities for both experiments (E) and simulation (S). In both approaches, step length showed an increasing trend as walking speed increased and higher step cadence is

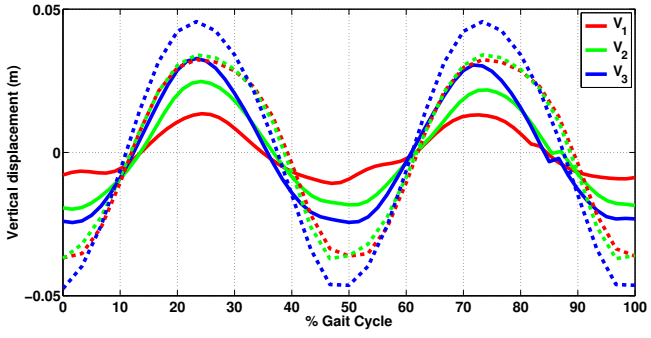


FIG. 8 – *Vertical displacement of COM during a GC. Solid line for experimental data, dashed line for simulation data.*

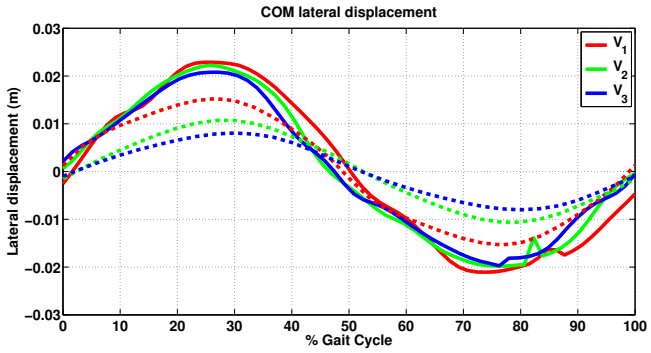


FIG. 9 – *COM mediolateral displacement during a GC. Solid line for experimental data, dashed line for simulation data.*

TABLE I – *Step characteristics across three gait velocities for experimental and simulation data. (E): experimental data, (S): simulation data.*

| Gait speed | Step length (cm) (E) | Step length (cm) (S) | Step width (cm) (E) | Step width (cm) (S) | step cadence ($s^{-1}$) (E) | step cadence ($s^{-1}$) (S) |
|---|---|---|---|---|---|---|
| $V_1$ | 56 | 59.2 | 11.4 | 11 | 1.79 | 1.69 |
| $V_2$ | 71.7 | 69 | 9.2 | 11.6 | 1.98 | 2.12 |
| $V_3$ | 80.4 | 76.2 | 8.5 | 11.7 | 2 | 2.11 |

obtained for faster walking velocities ($V_2$ and $V_3$) compared to low velocity. For simulation, step length and width results were close to those found in experiments.

### C. Hand's acceleration

Fig. 10 shows data related to acceleration parameters usually used in previous step length models. It is observed that vertical acceleration items have the same variation trend in terms of gait velocity. In both experimentation and simulation, these variables increase for faster gait velocities due to greater arm swing magnitude. The difference between experimental values and those of simulation is mainly due to the limited number of intermediate knots considered in simulation (two intermediate knots). Higher number of intermediate knots will be considered in future work in order to have smoother joint acceleration profiles (for shoulder and elbow joints)

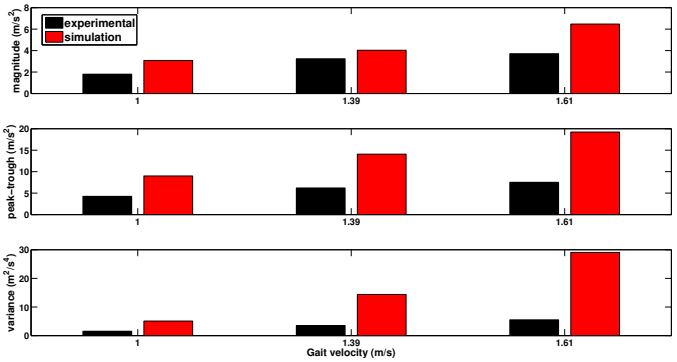


FIG. 10 – *The three items of hand's vertical acceleration (the magnitude, the difference of peak and trough, and the variance) according to different gait velocities.*

and consequently acceleration related characteristics closer to experimental ones.

## V. CONCLUSION AND FUTURE WORK

PDR is one of the most employed strategies to process inertial signals collected with handheld devices for navigation applications. In this process, most of parametric models used to estimate step length are only suitable for the most common human gait, since they only combine some step characteristics and physiological parameters. The accumulation of small errors in step length estimation leads to big errors in final positioning. Then, these models need frequent calibration based on empirical data that are costly to collect and do not cover the variety of human walking patterns. In this paper, we presented a realistic human gait model capable of coping with human gait variability. To check the validity of this model, we compared simulation outputs with motion capture data for one test subject. Results showed that the model reproduces the same fundamental patterns of walking found in experiments. Furthermore, The same variation trend of acceleration related items in function of gait velocity is observed for both approaches. Based on these results, simulation approach constitutes a novel manner of establishing relationships between user's displacement (e.g. step length) and signals sensed by handheld devices, and then more accurate step length estimation is foreseen.

Future work includes considering more time knots in optimization process in order to have acceleration characteristics closer to experimental ones. Experimental validation on several subjects with varied gait patterns is also targeted.

## REFERENCES


[1] M. Romanovas, V. Goridko, A. Al-Jawad, M. Schwaab, M. Traechtler, L. Klingbeil, and Y. Manoli, "A study on indoor pedestrian localization algorithms with foot-mounted sensors," in *2012 International Conference on Indoor Positioning and Indoor Navigation (IPIN)*, Nov 2012, pp. 1–10.

[2] F. Li, C. Zhao, G. Ding, J. Gong, C. Liu, and F. Zhao, "A reliable and accurate indoor localization method using phone inertial sensors," in *Proceedings of the 2012 ACM Conference on Ubiquitous Computing*. ACM, 2012, pp. 421–430.

[3] V. Renaudin, M. Susi, and G. Lachapelle, "Step length estimation using handheld inertial sensors," *Sensors*, vol. 12, no. 7, pp. 8507–8525, 2012.

[4] Y. Sun, H. Wu, and J. Schiller, "A step length estimation model for position tracking," in *2015 International Conference on Location and GNSS (ICL-GNSS)*, June 2015, pp. 1–6.

[5] J. Jahn, U. Batzer, J. Seitz, and J. G. Boronat, "Comparison and evaluation of acceleration based step length estimators for handheld devices," *International Conference on Indoor Positioning and Indoor Navigation (IPIN)*, pp. 1–6, 2010.

[6] M. Abid, V. Renaudin, Y. Aoustin, E. L. Carpentier, and T. Robert, "Walking gait step length asymmetry induced by handheld device," *IEEE Transactions on Neural Systems and Rehabilitation Engineering*, Accepted, In Press.

[7] S. H. Collins, P. G. Adamczyk, and A. D. Kuo, "Dynamic arm swinging in human walking," *Proceedings of the Royal Society B: Biological Sciences*, vol. 276, no. 1673, pp. 3679–3688, 2009.

[8] Y. Aoustin and A. M. Formalskii, "3D walking biped: optimal swing of the arms," *Multibody System Dynamics*, vol. 32, no. 1, pp. 55–66, 2014.

[9] J. B. Saunders, V. T. Inman, and H. D. Eberhar, "The major determinants in normal and pathological gait," *J Bone Joint Surg*, vol. 35-A, no. 3, p. 543, 1953.

[10] F. Prince, D. A. Winter, P. Stergiou, and S. Walt, "Anticipatory control of upper body balance during human locomotion," *Gait & Posture*, vol. 2, no. 1, pp. 19–25, 1994.

[11] J. Perry and J. Burnfield, *Gait Analysis: Normal and Pathological Function*. SLACK, 2010. [Online]. Available: https://books.google.fr/books?id=DICTQAAACAAJ

[12] J. Rose and J. Gamble, *Human Walking*, ser. LWW medical book collection. Lippincott Williams & Wilkins, 2006. [Online]. Available: https://books.google.fr/books?id=q6WrPwAACAAJ

[13] R. Dumas, L. Chèze, and J.-P. Verriest, "Adjustments to mcconville et al. and young et al. body segment inertial parameters," *Journal of Biomechanics*, vol. 40, no. 3, pp. 543–553, 2007.

[14] J. McConville, T. Churchill, I. Kaleps, C. Clauser, and J. Cuzzi, "Anthropometric relationships of body and body segment moments of inertia," Tech. Rep., 1980.

[15] J. Young, R. Chandler, C. Snow, K. Robinette, G. Zehner, and M. Lofberg, "Anthropometric and mass distribution characteristics of the adults female," Tech. Rep., 1983.

[16] M. J. D. Powell, *Variable Metric Methods for Constrained Optimization, Lecture Notes in Mathematics*. Springer, Berlin, 1977.

[17] C. Chevallereau and Y. Aoustin, "Optimal reference trajectories for walking and running of a biped robot," *Robotica*, vol. 19, no. 5, pp. 557–569, August 2001.

[18] H. J. Kim, Q. Wang, S. Rahmatalla, C. C. Swan, J. S. Arora, K. Abdel-Malek, and J. G. Assouline, "Dynamic motion planning of 3d human locomotion using gradient-based optimization." *Journal of biomechanical engineering*, vol. 130, no. 3, p. 031002, 2008.

[19] ULISS, http://www.ifsttar-geoloc.fr/index.php/en/equipment/44-uliss.

[20] M. L. Harris-Love, L. W. Forrester, R. F. Macko, K. H. C. Silver, and G. V. Smith, "Hemiparetic gait parameters in overground versus treadmill walking," *Neurorehabilitation and Neural Repair*, vol. 15, no. 2, pp. 105–112, 2001.

[21] J. Kim, H. Jang, D. Hwang, and C. Park, "A step, stride and heading determination for the pedestrian navigation system," *Positioning*, vol. 1, no. 8, p. 0, 2004.

[22] H. Weinberg, "Using the adxl202 in pedometer and personal navigation applications," *Analog Devices AN-602 application note*, 2002.

[23] I. Skog, P. Handel, J. O. Nilsson, and J. Rantakokko, "Zero-velocity detection - an algorithm evaluation," *IEEE Transactions on Biomedical Engineering*, vol. 57, no. 11, pp. 2657–2666, Nov 2010.

[24] H. Sakoe and S. Chiba, "A dynamic programming approach to continuous speech recognition," in *Proceedings of the Seventh International Congress on Acoustics, Budapest*, vol. 3. Budapest: Akadémiai Kiadó, 1971, pp. 65–69.